Current Science
CS 5 (1), 1200– 1212 (2025)
Received 26 **Nov** 2024 | **Revised 18 Dec.** 2024 | **Accepted 24 Jan**. 2025 | **Online Available 12 Feb** 2025
https://doi.org/ 10.52845/CS/2025-5-1-20

Current Science

Current Science

OPEN ACCESS

ISSN(O)2795-8639

ORIGINAL ARTICLE

Study on the Identification of Steel Slag Mixed in Fine Aggregate for Concrete Based on Color as Feature Elements

Mao Zhiyi[1,2], Wei Ziheng[3], Wang Tianlei[3], Zhang Lei[3,*], Yao Zhengying[4], Sun Qian[2], Wang Dongmei[2], Zhang Pengyu[1,2,*]

[1]Beijing Building Materials Academy of Sciences Research, State Key Laboratory of Solid Waste Reuse for Building Materials, Beijing 100041, China

[2]Tianjin Building Materials Science Research Academy *Co. Ltd*., Tianjin 300381, China

[3]School of Materials and Engineering, Tianjin Chengjian University, Tianjin 300384, China

[4]Tianjin Twenty-one Station Testing Technology *Co., Ltd.*, Tianjin 300381, China

Corresponding Author: Zhang Lei

Abstract

The frequent quality problems caused by steel slag concrete construction have received extensive attention and attention from the construction industry. How to effectively prevent the mixing of steel slag in raw materials for concrete has become a difficult problem faced by the current industry. In this paper, the phase and chemical composition of steel slag were analyzed to clarify the characteristic identification elements of steel slags and common fine aggregate for concrete. With the content of high-iron steel slag particles mixed in common fine aggregate increasing, the color of the mixed samples deepens, the diffuse absorption intensity in the visible light and near-infrared light range gradually increases, and the main peak position of the grey value gradually decreases. Through deep learning analysis, the precision and recall of TransUNet model for the mixed sample containing common fine aggregate and steel slag particles can reach more than 90.00%. Therefore, based on the color as a characteristic identification element, it can effectively identify whether fine aggregates is mixed with steel slag, so as to ensure the safety and stability of concrete structures.

Keywords: **Steel Slag; Fine Aggregate; Basic Properties; Identification Technology**

Introduction

With the vigorous development of infrastructure construction, the demand for concrete, as one of the most important civil engineering materials, is increasing year by year. Among them, aggregate is an key component of concrete, accounting for about 60% ~ 80% of the total volume[1-3]. The quality of aggregate not only affects the mechanical properties of concrete, but also plays a key role in construction performance and durability.

As the main by-product produced in the steelmaking process, the annual production of steel slag is about 120 million tons of steel slag in China [4]. The characteristics of steel slag include not only large fluctuations in chemical composition, mineral composition and particle size distribution, but also high hardness and low gelation, which makes its comprehensive utilization rate very low [5]. The accumulation of steel slag not only occupies a large amount of land resources, but also causes environmental pollution problems such as soil, water and air [6]. The chemical composition of steel slag mainly includes SiO_2, CaO, Fe_2O_3, *etc*., and its minerals include C_2S, C_3S, RO phase, which makes it possible to be used in building materials [7-10]. The steel slag was used to replace 30% of the coarse

aggregate for concrete, and the 28 d compressive strength was 16.79% higher than that of the control group [11]. Guo *et al.* [12] used steel slag sand to replace fine aggregate (0%, 10%, 20%, 30%, 40%) in different proportions, and studied the change rule of axial impact compression performance of steel slag sand concrete in detail. The incorporation of appropriate amount of steel slag can effectively improve the bond strength between aggregate and cement slurry, and gradually increase the compressive strength. However, when the steel slag content exceeds 20%, the unevenly distributed steel slag sand resulted in a decrease in the strength. Therefore, using an appropriate amount of steel slag instead of fine aggregate for concrete can not only improve its compressive strength and tensile strength, but also effectively reduce the permeability of water and harmful ions, thereby improving its durability [13].

The difference of steel slag smelting process and treatment process leads to many kinds of steel slag with the difference of composition and performance [14]. More importantly, steel slag contains a large amount of f-CaO and f-MgO, which can be accompanied by volume expansion during hydration process [15-16]. If steel slag is applied to concrete in a disordered and non-proportional manner, it is likely to seriously affect the volume stability of concrete and endanger the safety and stability of concrete structure [17-18]. Generally speaking, high activity f-CaO can undergo hydration reaction during curing process, medium activity f-CaO will undergo hydration reaction in boiling test, and low activity f-CaO can only undergo hydration reaction under autoclaved conditions [19]. Yang *et al.*[20] found that the compressive strength, splitting tensile strength and flexural strength of Engineered Cementitious Composites containing steel slag began to decrease after 90 d, especially when the content was 60%. Due to the volume expansion caused by the hydration of f-CaO, the sample completely is broken at 360 d. Morales *et al.* [21]analyzed the cracking and expansion deformation of a single-story R.C building at the connection between the wall and the floor, the wall and the column. Since a large amount of steel slag is used as aggregate in the concrete during the construction process, a large amount of f-CaO in steel slag is hydrated to cause volume expansion, which eventually leads to the expansion and cracking of the building structures. Due to the incorporation of insufficiently pretreated steel slag aggregate into the aggregate, a large number of bulging and cracking areas appear in the concrete walls, columns and roofs. It can be found that the cracks in the bulging and cracking areas radiate outwards from the center of dark or white aggregates with a particle size in the range of 2-5 mm, and the aggregate appears to pulverize as soon as it touches[22]. Therefore, it is strictly prohibited to mix inferior aggregates such as steel slag into the aggregate, which is very important to improve the quality assurance ability of concrete.

At present, concrete production enterprises usually distinguish steel slag and common fine aggregate according to the difference of color and morphology. However, with the increasing types of fine aggregates, the color and morphology are also more abundant, which makes it difficult to identify steel slag from fine aggregate based on experience, and the difficulty of identification is greatly increased. Chen *et al.* [23] obtained the morphological characteristics of steel slag concrete samples with different contents(3%, 6%, 9%) *via* industrial CT scanning. By setting a reasonable grey range of steel slag particles, the content of steel slag particles is calculated. However, CT equipment is expensive and the detection process is cumbersome, which is difficult to apply in practice. Xu *et al.* [24] summarized the analysis of the morphology, microstructure and internal structure of steel slag lithofacies by optical and electron microscopy in recent years, and clarified its optical characteristics. At the same time, the accuracy and limitations of XRF, QXRD, NMR, TG analysis, Rietveld refinement, titration, extraction and other methods for the detection of mineral composition and chemical composition of steel slag were compared. Teng *et al.*[25] added a squeeze and excitation attention mechanism to the ConvNeXt model and improved the ability to extract the color characteristics of steel slag sand mixture. After using the transfer learning training method, the prediction accuracy of the model for the replacement rate of steel slag sand is 92.64%, which provides a new idea for subsequent research.

Based on the above, this paper systematically analyzed the chemical composition, mineral

composition and macroscopic morphology of steel slag, and clarified the influence law of its composition-structure-property, so as to determine its characteristic identification elements. Subsequently, ultraviolet-visible diffuse absorption spectrum, grey value analysis and deep learning were used to quickly identify steel slag and commonly used fine aggregate, so as to obtain feasible detection technology, which can provide an important guarantee for avoiding the durability of concrete caused by the mixing of steel slag aggregate.

1. Experimental details

Steel slag sand (density of 2.78 g/cm^3) was taken from a steel plant in Dongli District, Tianjin. River sand (density of 2.60 g/cm^3, fineness modulus of 2.79) was collected from a river section in Tangshan, Hebei Province. Manufactured sand (density of 2.63 g/cm^3) was purchased from the building materials market. Barium sulfate (spectral purity) was provided by Shanghai Yien Chemical Technology *Co., LTD*. In order to be more suitable for practical application, the steel slag sand was configured according to the particle size distribution of the river sand, and the full-size steel slag of 5%, 10%, 15% and 20% was mixed with the common fine aggregate according to the volume substitution method.

The morphology of the samples was analyzed by ultra-depth-of-field microscope (VHX-600e, KEYENCE *Co., Ltd.*, Japan). The mineral composition of the samples was analyzed by X-ray diffractometer (D/MAX-Ultima IV, Rigaku *Co., Ltd.*). The chemical composition and their contents were determined by X-ray fluorescence spectrometer (ZSXPrimus II, Rigaku *Co., Ltd.*). UV-Vis-NIR spectrophotometer (LAMBDA750, PerkinElmer) was selected to measure the diffuse absorption intensity, and the scan range was 200-2500 nm. Image-J software (1.52a) was used to binarize the photographs and calculate their grey values.

The Pytorch environment is used to build Unet and TransUNet models for deep learning of steel slag identification. The encoder of UNet first performs three times of downsampling to extract features, and saves the corresponding pre-downsampling feature map as a jump connection. After three times of upsampling and after each upsampling, it can also be merged with the feature map of the corresponding size retained before. The difference between TransUNet and UNet is that in the encoder part, the feature map after three times of downsampling also needs to be encoded by the Transformer module. The data set is an image data set collected from mixed samples of self-made steel slag and commonly used fine aggregate under different light conditions and different angles. The precision, recall and $F_{1\text{-score}}$ are used as evaluation indicators to measure the detection effect of steel slag. The precision calculating by Formula 1 represents the correct data proportion of the positive samples predicted by the model. The recall rate represents the proportion of positive samples in the sample that predicts the correct data, and is calculated as shown in Formula 2. The $F_{1\text{-score}}$ can comprehensively reflect the precision and recall ability of the model. For each type of steel slag particles, FP represents the number of steel slag particles that are mistakenly detected, TP represents the number of steel slag particles that are correctly detected, and FN represents the number of steel slag particles that are missed.

$$\text{Precision}=TP/(TP+FP) \quad (1)$$

$$\text{Recall}=TP/(TP+FN) \quad (2)$$

$$F_{1\text{-score}}=2/(1/\text{Precision}+1/\text{Recall}) \quad (3)$$

2. Results and discussion

Table 1 shows the main chemical composition of steel slag sand, river sand and manufactured sand. The content of SiO_2 in river sand and manufactured sand is the highest, reaching 69.70% and 68.30%, respectively. The second is the content of Al_2O_3, which is 14.40%, 14.80%, respectively. The sum of SiO_2 content and Al_2O_3 content of the two is higher, both greater than 82.00%, indicating that the content of silicon-aluminum minerals is more. In addition, river sand and manufactured sand contain more K_2O, Na_2O and CaO, and there is almost no or little amount of MnO and P_2O_5. It is particularly noteworthy that the content of Fe_2O_3 in river sand and manufactured sand accounts for about 3.60% of the total mass, but that in steel slag sand can reach 24.60%. In the process of steel smelting, a

large amount of limestone needs to be added for desulfurization and dephosphorization so that the content of CaO in steel slag sand is high, about 33.80%. At the same time, limestone is mostly associated with dolomite or magnesite, resulting the content of MgO as high as 9.39% in steel slag sand. In addition, compared with river sand and manufactured sand, steel slag sand contains more MnO and P_2O_5, while less K_2O, Na_2O and Al_2O_3. In summary, steel slag sand contains a large amount of CaO, and heavy black metal elements such as Fe and Mn account for a relatively high proportion, but there are relatively high content of light elements such as Si and Al in river sand.

Table 1 Main chemical composition of steel slag sand, river sand and manufactured sand (*wt*%)

	SiO_2	CaO	MgO	Fe_2O_3	Al_2O_3	K_2O	Na_2O	P_2O_5	MnO
Steel slag sand	18.70	33.80	9.39	24.60	1.98	0.16	0.22	1.80	7.11
river sand	69.70	1.88	2.34	3.51	14.40	3.72	3.76	0.15	/
manufactured sand	68.30	1.58	0.86	3.64	14.80	6.63	2.41	0.16	/

Due to the influence of raw materials, steelmaking methods, alkalinity, cooling treatment and other factors, the mineral composition of steel slag is very complex, mainly containing calcite, magnetite and monticellite (Fig. 1). Among them, the iron element with high content in steel slag sand is mainly in the form of magnetite, and the calcium element is mainly in calcite and monticellite. River sand mainly contains quartz, albite and monticellite. The main mineral composition of the manufactured sand is quartz, potassium feldspar, muscovite, albite and so on. Therefore, river sand and manufactured sand are mainly composed of light-colored minerals such as quartz and albite, while steel slag sand contains dark-colored magnetite and other minerals.These mineral compositions result in the difference of color between steel slag sand and common fine aggregate, which will provide a theoretical basis for rapid identification of steel slag sand.

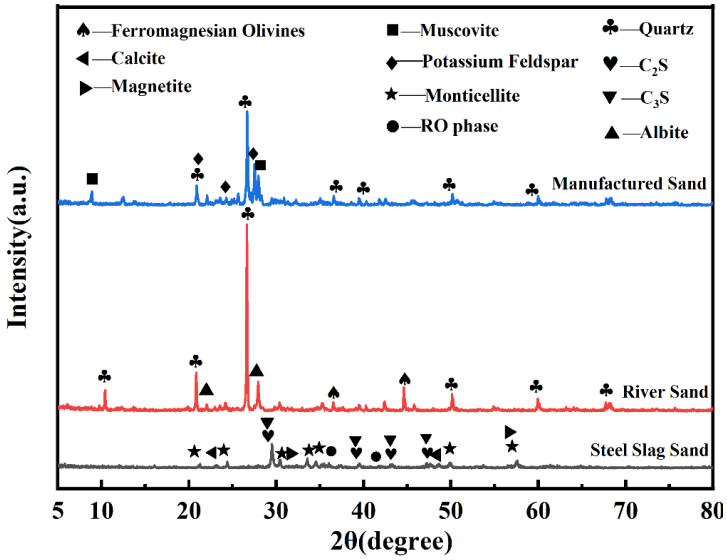

Figure 1 X-ray diffraction patterns of steel slag sand, river sand and manufactured sand

It can be seen from Fig. 2a that the shape of steel slag sand particles is irregular, and the surface is relatively rough and porous. This is mainly due to the overflow of water vapor and other gases inside the steel slag sand during the cooling process. Due to the long-term geological effects, the surface of river sand and manufactured sand particles is smooth and the structure is dense(Fig. 2b and 2c). From the color point of view, due to the high content of Fe and Mn in the steel slag sand, the color of most of its particles is darker. In the steelmaking stage, limestone is often added for desulfurization and dephosphorization, so the steel slag sand is composed of large white particles. The content of Si and Al elements in the river sand and manufactured sand is higher, and the

color is lighter.At the same time, river sand and manufactured sand contain a small amount of dark particles, which is mainly due to the enrichment of dark minerals such as iron minerals in the particles.

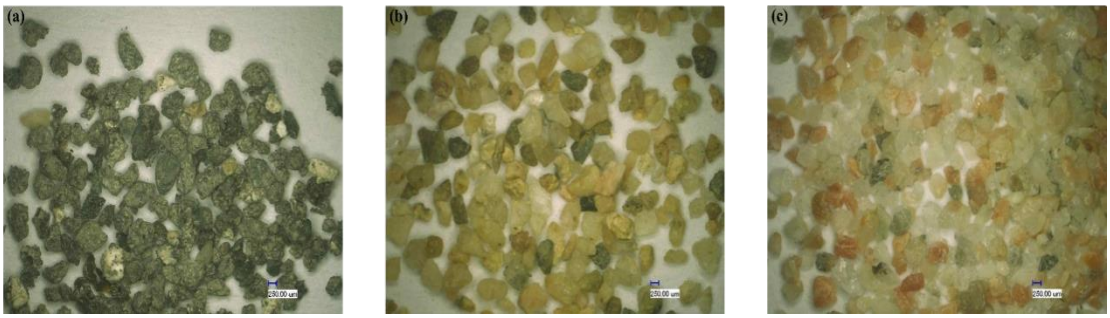

Figure 2 Ultra-depth-of-field microscope photos of Steel slag sand (a), river sand (b), manufactured sand (c)

It can be seen from Fig. 3a that the absorption intensities of river sand are low, while the intensities of steel slag sand are high. As the replacement rate of steel slag sand increases, the absorption intensity increases gradually. In the ultraviolet region, the samples show obvious absorption peaks, but the intensities are not much different, and there is no obvious rule. In the visible light range, the samples have almost no obvious absorption peak. At 745.0 nm, the fitting coefficient (R-square) of intensity and content is 0.96, showing a certain linear relationship(Fig. 3b). In the near-infrared region, the absorption intensities in the wavelength of 855.0 nm shows a good linear relationship with the content, and the R-square is 0.96 (Fig. 3c). At 2295.0 nm, the R-square of absorption intensity and content is 0.97, showing a good linear relationship (Fig. 3d). Therefore, compared with the ultraviolet light range, steel slag mixed with river sand is more suitable for effective identification by using the absorption intensity of visible light, near-infrared region.

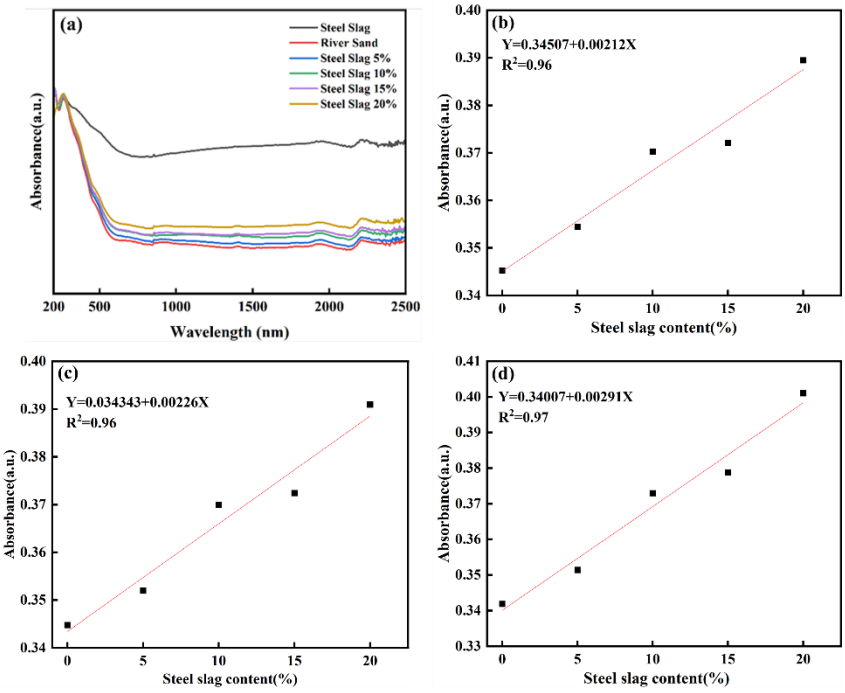

Figure 3 The diffuse absorption spectrum curve of adding steel slag sand (5%, 10%, 15%, 20%) to the river sand according to the volume substitution method (a) and the linear relationship between the content and the absorption intensity at 745.0 nm (b), 855.0 nm (c), 2295.0 nm (d)

It can be seen from Fig. 4 that the absorption intensities of manufactured sand with the same

particle size are lower, while the intensities of steel slag sand are higher. The absorption intensities of the sample obtained by replacing the manufactured sand of steel slag sand gradually increases with the increase of content. Similarly, in the ultraviolet range, the absorption intensity and content of the sample do not show obvious regularity. The absorption intensities at 745.0 nm, 855.0 nm and 2295.0 nm are selected to fit the content, and the R-square are 0.97, 0.96 and 0.98, respectively, showing a good linear relationship. Therefore, compared with the ultraviolet light range, the steel slag mixed in the manufactured sand can also be effectively identified by the absorption intensity in the visible light, near-infrared region.

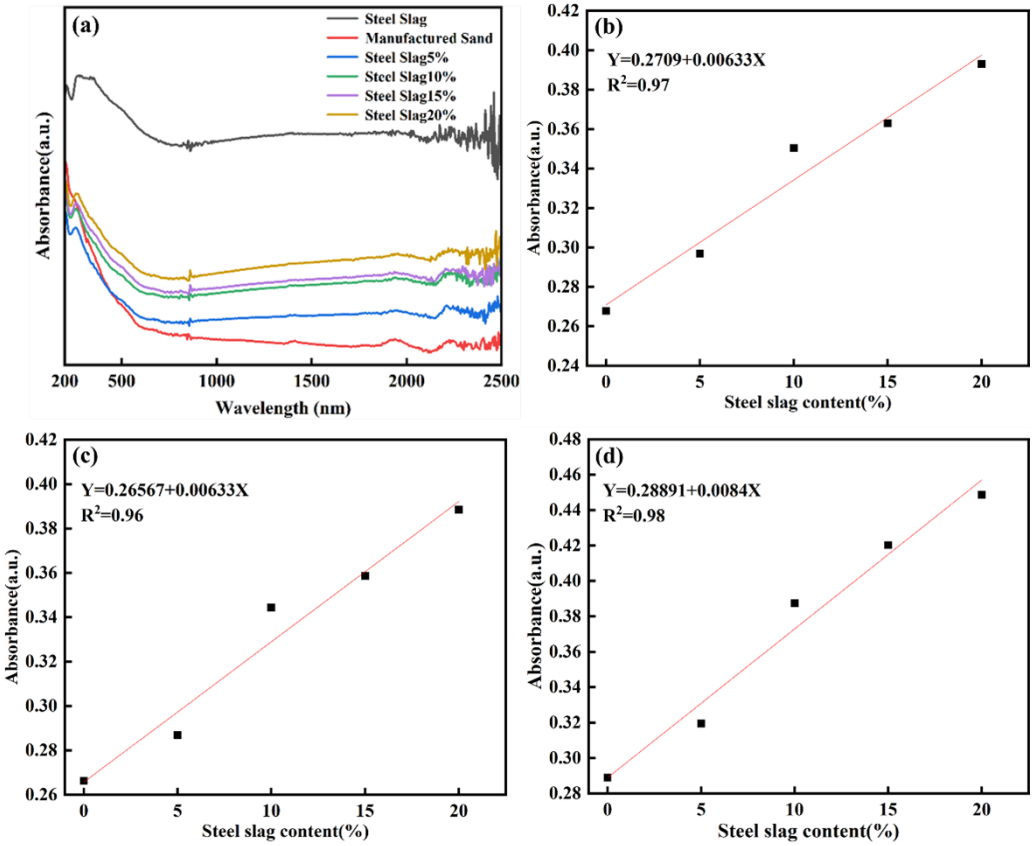

Figure 4 The diffuse absorption spectrum curve of adding steel slag sand (5%, 10%, 15%, 20%) to the manufactured sand according to the volume substitution method (a) and the linear relationship between the content and the absorption intensity at 745.0 nm, (b), 855.0 nm (c), 2295.0 nm (d)

Fig. 5 shows the ultra-depth-of-field microscope photos and grey value analysis of steel slag sand (a, b), river sand (c, d) and manufactured sand(e, f). Due to the high content of Fe_2O_3 in steel slag sand and 7.11% of MnO, the color is darker. After binarizing the photo, the calculated Mode value is 73, which represents the position where the grey value is the most concentrated in the picture, that is, the main peak position. The color of the river sand is lighter, with a Mode value of 107. The color of manufactured sand is the lightest, and its Mode value is 126. Therefore, the differences in the chemical composition and mineral composition of the particles make the samples show color changes, which in turn causes changes in grey value.

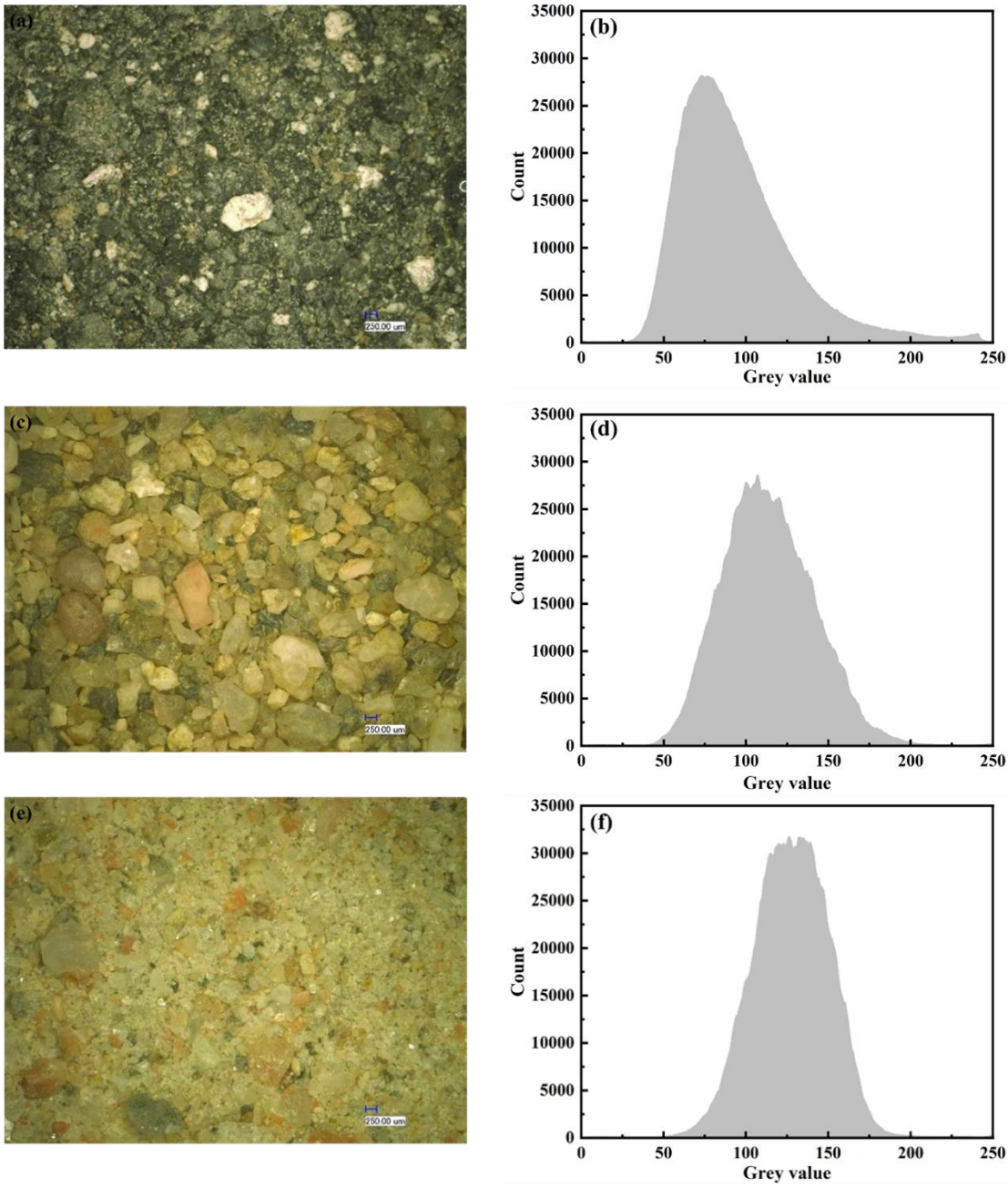

Figure 5 Ultra-depth-of-field microscope photos and grey values of steel slag sand (a, b), river sand (c, d) and manufactured sand(e, f)

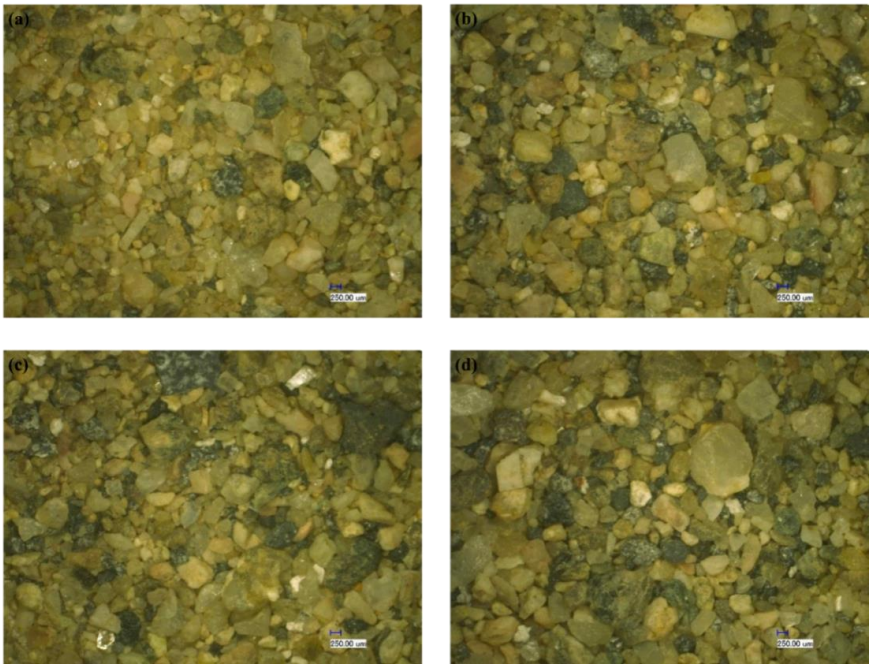

Figure 6 Ultra-depth-of-field microscope photos of steel slag sand and river sand with different contents (a: 5%, b: 10%, c: 15%, d: 20%)

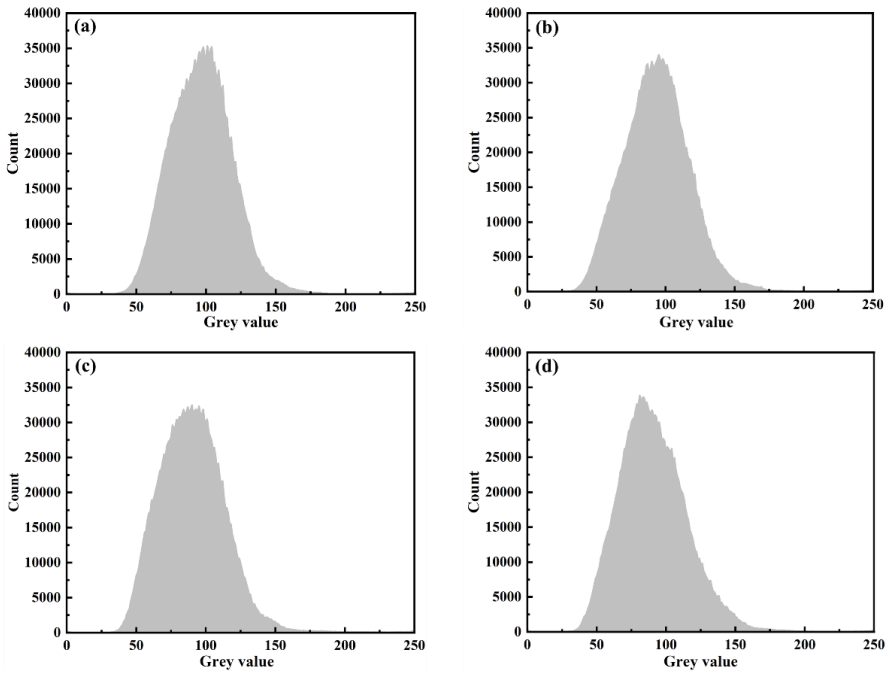

Figure 7 The grey values of steel slag sand and river sand with different contents (a: 5%, b: 10%, c: 15%, d: 20%)

With the increase of the content, the number of dark particles in the field of vision increases, resulting in the main peak position of the grey value shifting to the left, and the grey value gradually decreases (Fig. 6 and Fig. 7). The Mode value of river sand mixed with 5% steel slag sand is 101, the Mode value of river sand mixed with 10% steel slag sand is 95, the Mode value of river sand mixed with 15% steel slag sand is 90, and the Mode value of river sand mixed with 20 % steel slag sand is 81. It can be seen that with the increase of steel slag sand content, the number of dark particles increases and the grey value decreases gradually.

The content of Fe and Mn in steel slag sand is the larger, accounting for 24.6% and 7.11%, while the content of aluminosilicate minerals in manufactured sand is more, the sum of SiO_2 content and Al_2O_3 content is more than 82%. As shown in Fig. 8 and Fig. 9, the color of steel slag

sand is much deeper than that of manufactured sand. The Mode value of the manufactured sand mixed with 5% steel slag sand is 111, the Mode value of the manufactured sand mixed with10% steel slag sand is 106, the Mode value of the manufactured sand mixed with 15% steel slag sand is 100, and the Mode value of the manufactured sand mixed with 20% steel slag sand is 91. Therefore, by analyzing the gray value of the samples photographs, it can be judged to a certain extent that the common fine aggregates are mixed with steel slag.

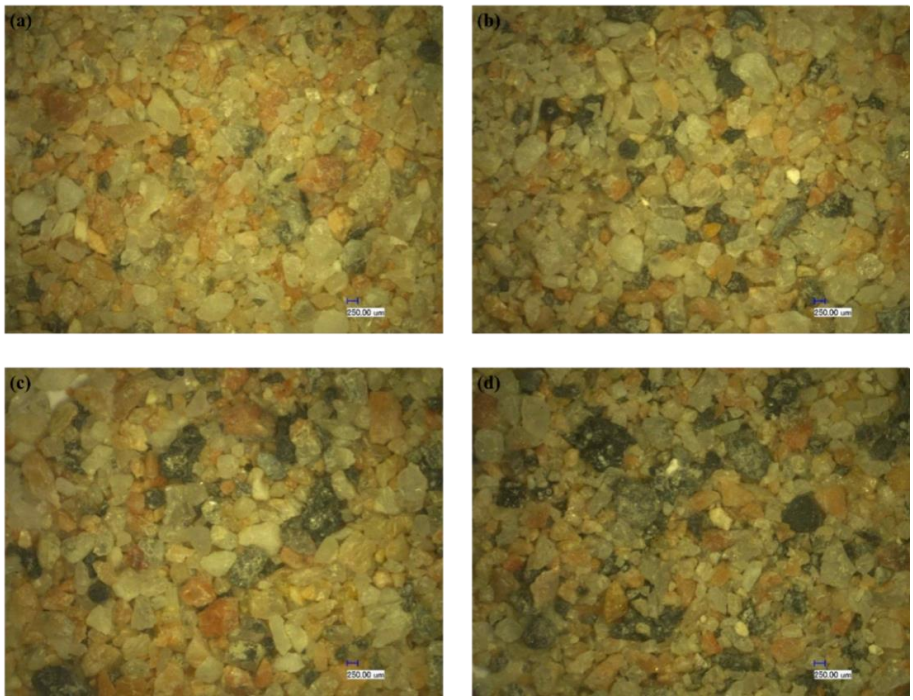

Figure 8 Ultra-depth-of-field microscope photos of steel slag sand and manufactured sand with different contents (a: 5%, b: 10%, c: 15%, d: 20%)

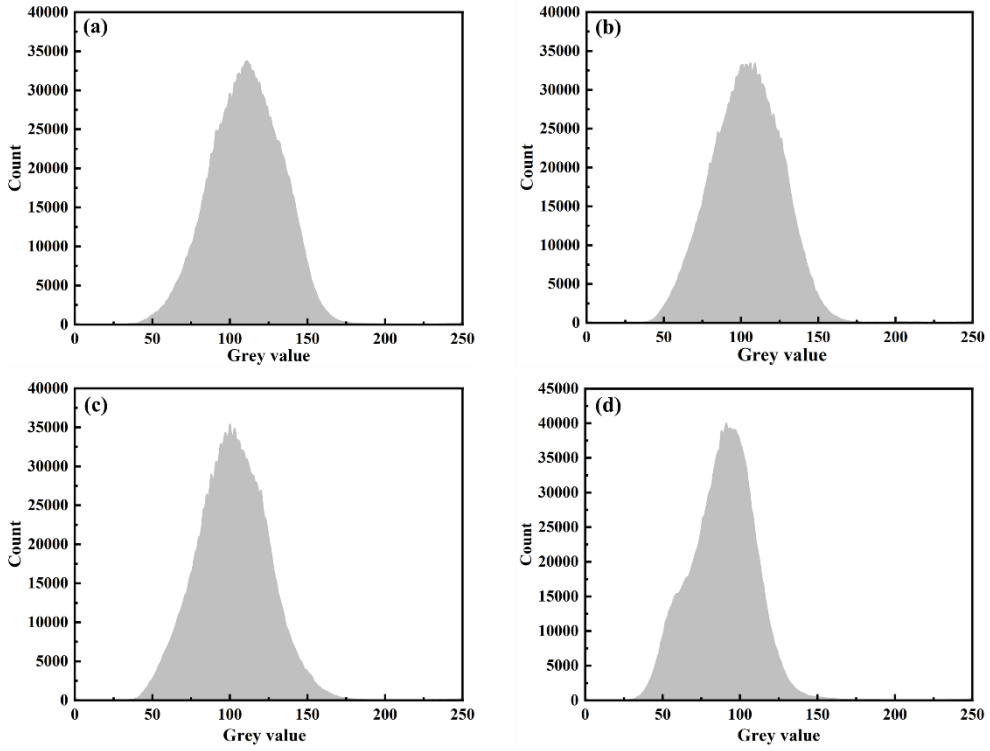

Figure 9 The grey values of steel slag sand and manufactured sand with different contents (a: 5%, b: 10%, c: 15%, d: 20%)

Based on the differences in the color of steel slag and river sand particles, the UNet and TransUNet model were used to perform deep learning on the collected images. Due to the unique chemical composition and mineral composition of steel slag, the color of its particles is obviously different from that of commonly fine aggregate particles, so as to achieve the effect of rapid identification. As shown in Fig. 10 and Fig. 11, the particles in the images can be clearly divided into two categories by using the UNet and TransUNet model, among which the green is steel slag sand particles and the red is common fine aggregate particles, in order to intuitively and quickly identify the steel slag mixed in the aggregate. When the UNet model is selected to identify the mixed samples, some areas in the same particle are classified into steel slag, and other areas are classified into common fine aggregate. This is mainly due to the fact that the common fine aggregate contains a certain amount of iron compounds, which makes the color of the particles close to the color of the steel slag particles, so that the model is not ideal for the identification of complex particles. When the Tranformer module is introduced into the UNet model, the ability to understand the global context is enhanced, thus avoiding the misclassification of single particles into two categories. When the photograph of mixed samples about steel slag replacing river sand are loaded into the UNet model for recognition, the precision is 87.11% and the recall is 87.64%, while the precision using TransUNet model can be improved to 93.15% and the recall rate can also reach 95.40% (Table 2). Similarly, when the Tranformer module is introduced into the UNet model, the precision and recall are increased to more than 90%. Therefore, compared with the UNet model, the precision and recall of the TransUNet model are higher, reaching more than 90.00%, indicating that the detection effect is better, and the steel slag mixed into the common fine aggregate can be identified more quickly and accurately.

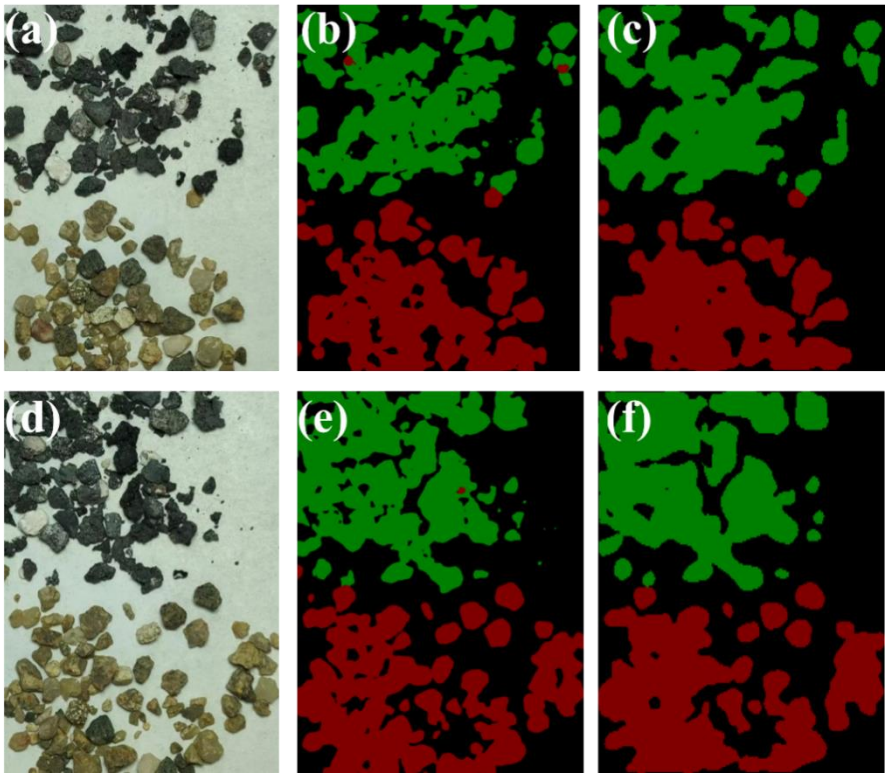

Figure 10 The deep learning recognition results of the mixed samples of steel slag and river sand (a,d: original photograph, b, e :UNet model recognition results, c, f: TransUNet model recognition results)

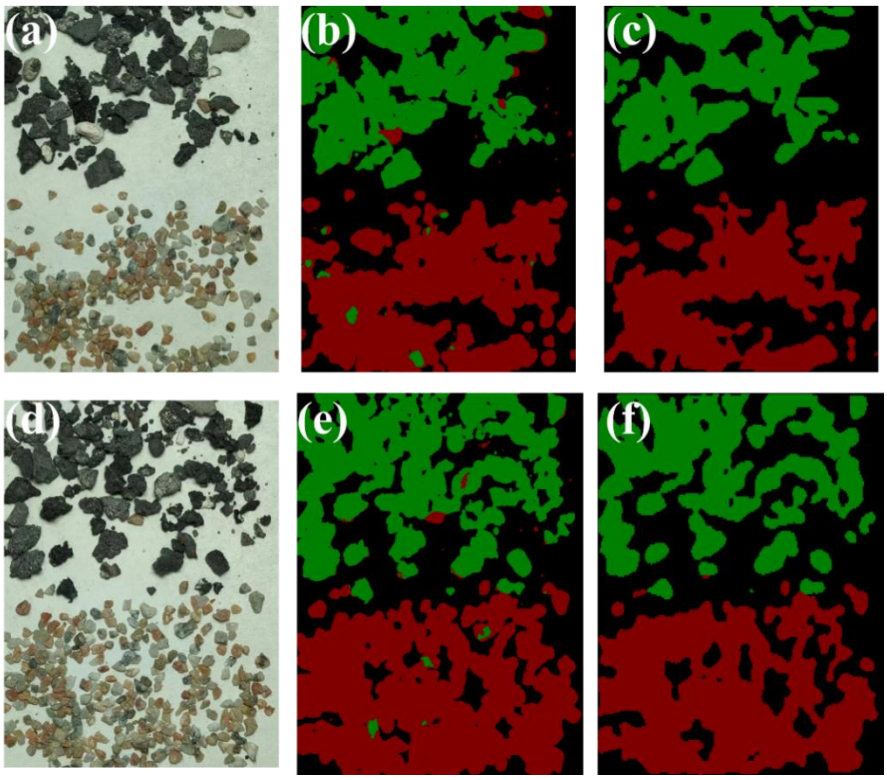

Figure 11 The deep learning recognition results of the mixed samples of steel slag and manufactured sand(a,d: original photograph, b, e :UNet model recognition results, c, f: TransUNet model recognition results)

Table 2 The deep learning recognition results of the mixed samples of steel slag and common fine aggregates

Sample	Model	Precision (%)	Recall(%)	$F_{1\text{-score}}$
Mixed samples of steel slag and river sand	UNet	87.11	87.64	87.37
	TransUNet	93.15	92.36	92.75
Mixed samples of steel slag and manufactured sand	UNet	84.26	85.15	84.70
	TransUNet	90.07	90.79	90.43

Conclusion

The phase composition, chemical composition and macroscopic morphology of steel slag sand and river sand were characterized. It is found that the content of iron in steel slag sand is 24.60%, which mainly exists in the form of magnetite, resulting in the color of steel slag particles showing dark grey or even black. There are mainly light or even colorless minerals such as quartz and feldspar in common fine aggregates, making their particles white, yellow or even transparent. Therefore, due to the change of chemical composition and mineral composition, the color of steel slag sand and river sand particles is obviously different, which can be used as the characteristic identification elements of steel slag sand and common fine aggregate. With the increase of steel slag content, the color of the mixed samples gradually deepened. Based on the color difference characteristics, the grey value decreases linearly, and the absorption intensity at 745.0 nm, 855.0 nm and 2295.0 nm increases linearly. At the same time, through the images recognition of UNet model and TransUNet deep learning model, the precision and recall of the TransUNet model can reach a maximum of more than 90.00%. Therefore, based on the composition characteristics of fine aggregate, the convenient and quick detection technology of steel slag sand mixed in common fine aggregate is determined, which provides technical guarantee for avoiding the durability problem caused by steel slag sand

mixed in concrete.

Acknowledgments: This study was partially supported by the National Natural Science Foundation of China (Grant Nos. 52078321, 52178265).

References

1. Mohammed T, Mahmood A, Zunaied-Bin-Harun M, *et al*. Destructive and non-destructive evaluation of concrete for optimum sand to aggregate volume ratio[J]. Frontiers of Structural and Civil Engineering, 2021, 15(6): 1400-1414. https://doi.org/10.1007/s11709-021-0779-8
2. Mohammed T, Bin Harun M, Joy J. Effect of sand-to-aggregate volume ratio on durability of concrete[J]. Innovative Infrastructure Solutions, 2022, 7(5): 318. https://doi.org/10.1016/j.conbuildmat.2020.118046
3. Kumar L, Thanappan S, Mekonnen E, *et al*. Effect of fly ash and sand stone slurry on mechanical properties of concrete materials[J]. Materials Today: Proceedings, 2021, 45: 2878-2882. https://doi.org/10.1016/j.matpr.2020.11.856
4. Wang J, Fu H, Yan X, *et al*. Research status of comprehensive utilization of steel slag[J]. China Nonferrous Metall, 2021, 50: 77-82.
5. Gao W, Zhou W, Lyu X, *et al*. Comprehensive utilization of steel slag: A review[J]. Powder Technology, 2023, 422: 118449. https://doi.org/10.1016/ j.powtec.2023.118449
6. Huo B, Li B, Huang S, *et al*. Hydration and soundness properties of phosphoric acid modified steel slag powder[J]. Construction and Building Materials, 2020, 254: 119319. https://doi.org/10.1016/j.conbuildmat.2020.119319
7. Baalamurugan J, Kumar V G, Padmapriya R, *et al*. Recent applications of steel slag in construction industry[J]. Environment, Development and Sustainability, 2024, 26(2): 2865-2896. https://doi.org/10.1007/s10668-022-02894-3
8. Fang Y, Shan J, Wang Q, *et al*. Semi-dry and aqueous carbonation of steel slag: Characteristics and properties of steel slag as supplementary cementitious materials[J]. Construction and Building Materials, 2024, 425: 135981. https://doi.org/10.1016/j.conbuildmat.2024.135981
9. Li Z, Shen A, Yang X, *et al*. A review of steel slag as a substitute for natural aggregate applied to cement concrete[J]. Road Materials and Pavement Design, 2023, 24(2): 537-559. 10.1080/14680629.2021.2024241
10. Xue P, Xu A, He D, *et al*. Research on the sintering process and characteristics of belite sulphoaluminate cement produced by BOF slag[J]. Construction and Building Materials, 2016, 122: 567-576. https://doi.org/10.1016/j.conbuildmat. 2016.06.098
11. Kashyaop R, Saxena M, Gautam A, *et al*. A study on enhancing mechanical properties of concrete with steel slag for sustainable construction[J]. Journal of Building Pathology and Rehabilitation, 2024, 9: 130. https://doi.org/10.21203/ rs.3.rs-4418406/v1
12. Guo Y, Xie J, Zheng W, *et al*. Effects of steel slag as fine aggregate on static and impact behaviours of concrete[J]. Construction and Building Materials, 2018, 192: 194-201. https://doi.org/10.1016/j.conbuildmat.2018.10.129
13. Afaque M, Khan R, Roy S. Durability and strength enhancement in concrete using steel slag as fine aggregate replacement[J]. Materials Circular Economy, 2024, 6(1): 46. https://doi.org/10.1007/s42824-024-00140-x
14. Liu X, Zhang C, Yu H, *et al*. Research on the properties of steel slag with different preparation processes[J]. Materials, 2024, 17(7): 1555. https://doi.org/ 10.3390/ma17071555
15. Hou J, Chen Z, Liu J. Hydration activity and expansibility model for the RO phase in steel slag[J]. Metallurgical and Materials Transactions B, 2020, 51: 1697-1704. https://doi.org/10.1007/s11663-020-01847-3
16. Imashuku S, Tsuneda H, Wagatsuma K. Rapid and simple identification of free magnesia in steelmaking slag used for road construction using cathodoluminescence[J]. Metallurgical and Materials Transactions B, 2020, 51: 27-34. https://doi.org/10.1007/s11663-019-01724-8
17. Long Q, Zhao Q, Gong W, *et al*. Effect of magnesian-expansive components in steel slag on the volume stability of cement-based materials [J]. Materials, 2023, 16(13): 4675. https://doi.org/10.3390/ma16134675
18. Kuo W, Shu C, Han Y. Electric arc furnace oxidizing slag mortar with volume stability for rapid detection[J]. Construction and building materials, 2014, 53: 635-641. https://doi.org/

10. 1016/ j.conbuildmat.2013.12.023
19. Chen T, Weng Y, Liu Y, *et al*. Calculation of f-CaO Hydration ratio in steel slag based on mathematical model of hydration expansion of steel slag-cement cementitious materials[J]. Jom, 2023, 75(12): 5243-5251. https://doi.org/ 10.1007/ s11837-023-05946-9
20. Yang Z, Xiong X, Li K, *et al*. Long-term volume stability of ECC containing high-volume steel slag[J]. Cement and Concrete Composites, 2024,145:105352. https://doi.org /10.1016/j.cemconcomp.2023.105352
21. Morales, E. Structural and functional distress due to slag expansion[C]. International Conference on Case Histories in Geotechnical Engineering, Louis, MO, USA, 1993: 10. https://api.semanticscholar.org/CorpusID:136052825
22. Zhang L, Li Z, Yin L H, *et al*. Detection and renovation for heave and burst of a slag concrete structure[J]. Building Structures, 2021, 51(S1): 1639-1642. (in Chinese)
23. Chen C, Li Z, Pan W, *et al*. Application of industrial CT to identify mixed steel slag particles in concrete[J]. Journal of Building Materials, 2024, 27(04): 343-349. (in Chinese) https://doi.org/10.3969/j.issn.1007-9629.2024.04.008
24. Xu Y, Lv Y, Qian C. Comprehensive multiphase visualization of steel slag and related research in cement: Detection technology and application[J]. Construction and Building Materials, 2023, 386: 131572. https://doi.org/10.1016/j.conbuildmat. 2023.131572
25. Teng S, Zhu L, Li Y, *et al*. ConvNeXt steel slag sand substitution rate detection method incorporating attention mechanism[J]. Scientific Reports, 2023, 13(1): 10593. https://doi.org/10.1038/s41598-023-37676-y